Topology and dynamics of streakline on the mixing boundary of two-dimensional chaotic flow induced by a rotationally reciprocating anchor impeller

Hirose, Haruna
Komoda, Yoshiyuki
Horie, Takafumi
Ohmura, Naoto

(Citation)
Journal of the Taiwan Institute of Chemical Engineers,131:104213

(Issue Date)
2022-02

(Resource Type)
journal article

(Version)
Accepted Manuscript

(URL)
https://hdl.handle.net/20.500.14094/90009290

Topology and dynamics of streakline on the mixing boundary of two-dimensional chaotic flow induced by a rotationally reciprocating anchor impeller

Haruna Hirose[1], Yoshiyuki Komoda[1]*, Takafumi Horie[2], Naoto Ohmura[1]

[1] Department of Chemical Science and Engineering, Kobe University, 1-1Rokkodai-cho, Nada, Kobe, Hyogo 657-8510, Japan

[2] Department of Chemical Engineering, Graduate School of Engineering, Osaka Prefecture University, 1-1Gakuen-cho, Naka-ku, Sakai, Osaka 599-8531, Japan

* Corresponding author

E-mail: komoda@kobe-u.ac.jp

Phone number: +81-78-803-6189

Abstract

Background

A rotationally reciprocating impeller separates the horizontal cross-section of the vessel into two mixing regions under a laminar flow regime. In this study, we investigated the separation mechanism from the dynamics of the streakline on the boundary.

Methods

The stretching behavior of the streakline on the universal boundary of active mixing regions was successfully visualized by injecting tracer fluid from a specific position.

Findings

The elongational rate of streakline proportionally increased with the increase in Reynolds number. Besides, the linear component of the elongation rate drastically changed at

$Re \sim 10$ due to the bending of the boundary. Compared with other chaotic mixing flows, we proved that tracer particles are enclosed in turnstile lobes at the hyperbolic fixed point at the wall, transported on the boundary, namely separatrix, to the mixing shaft being another hyperbolic fixed point, and then distributed evenly into both mixing regions. It was concluded that the boundary becomes wavy at $Re > 10$, which increases the area of turnstile lobes to enhance fluid transportation between two mixing regions.

Keywords

Laminar chaotic mixing; Separatrix; Streakline; Visualization

1. Introduction

Mixing using a mechanically rotating impeller is an essential unit operation widely used in industrial processes. In most practical processes, fluid mixing usually occurs in a turbulent regime by rotating the impeller at a higher speed. However, for fluids containing shear-sensitive substances, the rotational speed of the impeller may be limited to a low range. Consequently, the hydrodynamic condition in a vessel becomes laminar, where mixing performance is typically lower than that in a turbulent flow. Numerous works have been conducted to improve mixing performance in the laminar regime. One of the common strategies is to make impeller geometries more complicated. However, in the uni-directional rotating system that is mechanically more stable, the stable flow structure results in insufficient mixing performance, such as forming isolated mixing regions. The time-periodic motion of the impeller is thus another approach to change the whole flow domain into chaos, which enhances mixing performance even in the laminar regime.

Chaotic mixing has attracted considerable attention due to its high mixing efficiency, even in laminar regimes. Ottino and Leong experimentally demonstrated that periodical perturbation in the wall velocity significantly enhances fluid mixing in a cavity flow [1]. They indicated that the random and unpredictable motion causes a remarkable mixing performance in a time-periodic flow. In a chaotic flow, the stretching and folding motion leads to an exponential increase in the surface area of fluid elements. In the time-periodic Bénard convection, a typical model of chaotic mixing, the intersection of stable and unstable manifolds forms turnstile lobes by perturbing the cell boundary. These lobes carry fluid particles in one of the cells to the hyperbolic fixed point, taking complex arrangements. Then, the fluid particles propagate the other unit cells, which is the

mechanism of the high efficiency of chaotic mixing in laminar flow [2].

In stirred vessels, the periodic perturbation similarly induces chaotic mixing [3]. Lamberto et al. reported that time-dependent impeller rotation notably improves mixing performance in the laminar region [4]. After his work, many researchers have investigated the effect of time-dependent rotation of the impeller on mixing, such as changing rotational speed and direction [5, 6, 7, 8]. The reciprocating motion is another time-dependent protocol leading to chaotic mixing in a stirred vessel. Komoda et al. [9] and Hirata et al. [10] used a vertically reciprocating disk impeller and elucidated that the vortices near the impeller have a significant effect in accomplishing an excellent chaotic mixing performance.

We adopted the reciprocating protocol to the impeller rotation and proposed a rotationally reciprocating mixing, where an impeller slowly rotates back and forth in half rotations [11]. Senda et al. [12, 13] experimentally visualized the streakline in the horizontal cross-sectional plane of the vessel using a plate impeller. They reported that the stretching and folding fluid elements make excellent mixing possible even at low rotational speeds. As decreasing the Reynolds number, the fluid flow becomes two-dimensional without distinctive vertical flow. At the Reynolds number below criteria, the circular cross-section of the agitated vessel consists of two distinct mixing regions and a pair of central poor mixing regions. We then changed from a large plate to an anchor impeller and found that it intensified the fluid flow through the impeller clearance near the mixing shaft and eliminated the poor mixing regions. However, we still observed the separated two mixing regions. Therefore, understanding the separation mechanism by the rotationally reciprocating anchor impeller is necessary to accomplish the widespread mixing in the entire cross-section.

In the two-dimensional time-periodic flow system, the pairs of stable and unstable manifolds are the centerpiece of mixing. Although the stable manifold is not visible, the unstable manifold can be experimentally visualized as the streakline by periodic observation. The visualized unstable manifold has fundamental characteristics to understand the mechanism of chaotic mixing, i.e., 1) it has a time-independent property when it was observed periodically, and 2) is the template of the mixing pattern [3]. In addition, the mixing pattern reaches the configuration of streakline in shape.

The main goal of this study was therefore to reveal the mechanism of the separation of the active mixing regions in the horizontal cross-sectional plane in the vessel using a rotationally reciprocating anchor impeller. We observed the mixing pattern in detail and found the boundary separating the mixing regions. Then the boundary was visualized by injecting tracer fluid from a specific position. We classified the topology of the streakline elongating on the boundary and analyzed the elongation rate. Finally, the separation mechanism was discussed based on the theory of chaotic mixing.

2. Experiment

Fig. 1 illustrates the experimental setup. An anchor impeller is placed in the center of a flat-bottomed cylindrical vessel. Both of them are made of transparent acrylic resin. The vessel with an inner diameter of 80 mm is filled with aqueous glycerol solution of various concentrations to adjust the Reynolds number described later. The anchor impeller has a diameter of 60 mm and a blade width of 20 mm. The impeller has a height and thickness of 80 and 2 mm, respectively. The anchor impeller rotates back and forth using a stepper motor and a motion control board so that the angular position ϕ is

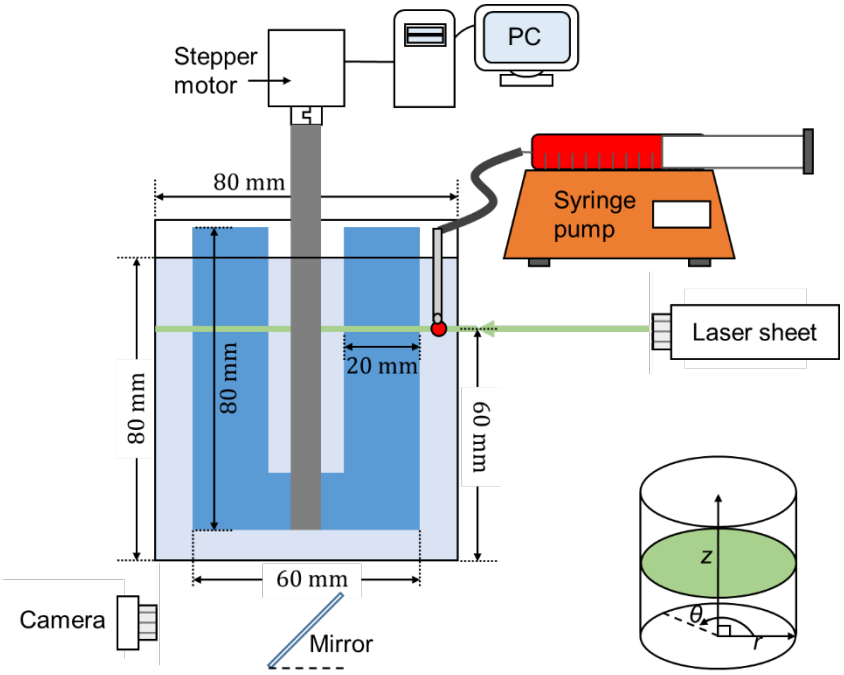

Fig. 1 Experimental apparatus.

represented by Eq. (1). Therefore, the angular velocity ω also changes as a sinusoidal function expressed in Eq. (2).

$$\phi(t) = A\{1 - \cos(2\pi t/T)\} \tag{1}$$

$$\omega(t) = 2\pi A/T \sin(2\pi t/T) \tag{2}$$

where A and T are the amplitude and period of the rotational reciprocation of the impeller. In the present study, they are constant at $A = \pi/2$ and $T = 4$ s similar to the previous work [12].

The streakline is visualized by injecting tracer fluid from a specific point in a horizontal cross-section (r-θ plane), which is 60 mm from the bottom and 20 mm below the liquid level. The tracer fluid is the glycerol solution, identical to the working fluid, containing 9 ppm Rhodamine B (Wako Pure Chemical Industries, Ltd.). The tracer fluid is continuously injected at 1.5 mL/min using a syringe pump (IC3210, KD Scientific Inc.)

and a syringe needle. A horizontal sheet of laser light is irradiated at the same height as the tracer injection point, and the stretching behavior of tracer fluid is recorded by a digital camera (FDR-AX700, Sony Marketing Inc.) through a mirror placed under the vessel. All the experiments are conducted at the Reynold number, defined by $Re\ (=\rho(4A/2\pi T)d^2/\mu)$, below 17, which corresponds to the laminar region. Here, ρ and μ represent the density and viscosity of the fluid, respectively.

3. Results and Discussion

3.1 Visualization of mixing pattern

We visualized the mixing pattern as the stretching process of streakline by injecting tracer fluid from a position; $r = 3.1$ cm and $\theta = 90°$. Since the impeller tip passes by the injection point at the highest peripheral speed, the tracer fluid is expected to be stretched significantly, and the streakline will promptly terminate to the final mixing pattern. The upper images in Fig. 2 describe the streakline in the first cycle after the injection of tracer fluid at $Re = 9.5$, where the layered streakline is confined in a semi-

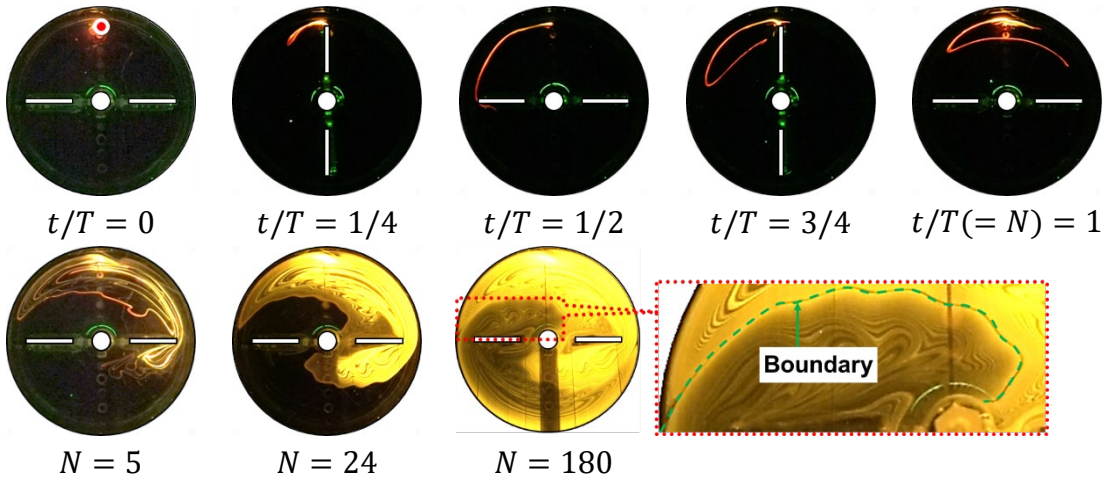

Fig. 2 Stretching behavior of the streakline and separation of mixing region ($Re = 9.5$).

circle region and the separation of mixing pattern is observed for a rotationally reciprocating plate impeller [12]. First, the streakline is stretched mainly along the wall of the vessel when the impeller tip passes by the injection point. However, after the impeller changes the rotational direction, the streakline is folded and forms a single layer. Under this condition, the streakline is stretched only within a semi-circle containing the injection point. This stretching behavior is almost the same as that observed for a plate impeller.

After sufficient cycles of reciprocation, the streakline converges to a specific pattern. To clarify the converging process of the streakline, the bottom images in Fig. 2 show the time series of the streaklines at the end of reciprocation. The tracer fluid injected is stretched along the wall in each half-cycle, which produces the layer structure of the streakline. With the increase of reciprocation cycle N $(= t/T)$, the number of layers increases, and the shape of the mixing pattern emerges gradually. However, many layers of streakline fill the mixing pattern, but the outline does not change further $(N = 24)$. As a result, fluid mixing proceeded only in the distinctive C-shaped region. However, after very long cycles $(N = 180)$, the tracer fluid expands to the other C-shape region though only a tiny portion of tracer fluid seems to enter the region. Additionally, those C-shape regions have the same shape and are symmetrical to the mixing shaft. We found that tracer fluid did not fill out the boundary of two C-shape regions, indicated by a green dashed line, as shown in the enlarged view of Fig. 2. The boundary of mixing regions changes the shape with Reynold number, but the separation of mixing regions was observed at all Reynolds numbers investigated ($Re < 17$). The anchor impeller did not produce a pair of isolated mixing regions, which is formed by the plate impeller. However, the separation of mixing regions is not avoidable even for the anchor impeller.

3.2 Visualization of the boundary of mixing regions

Ohmura et al. investigated the separation of the active mixing region and isolated mixing regions in a laminar chaotic mixing. They pointed out that the topology of their boundary or the stretching behavior of streakline is helpful to clarify the mechanism of chaotic mixing in a stirred vessel [14]. Thus, the present work focuses on the streakline elongating on the boundary of two distinctive mixing regions. Although the mixing region deforms and moves with the impeller motion, as shown in Fig. 3, one of the mixing regions always includes the tracer injection point, and consequently, the streakline expands only in the region. Therefore, to observe the dynamics of streakline on a moving boundary, it is necessary to either move the injection point with the boundary or find a stable point on the boundary that does not move regardless of impeller motion. However, since the shape of the boundary changes with time and the position relative to the impeller plate is not stable, the injection point rotating with the impeller is not acceptable for the purpose.

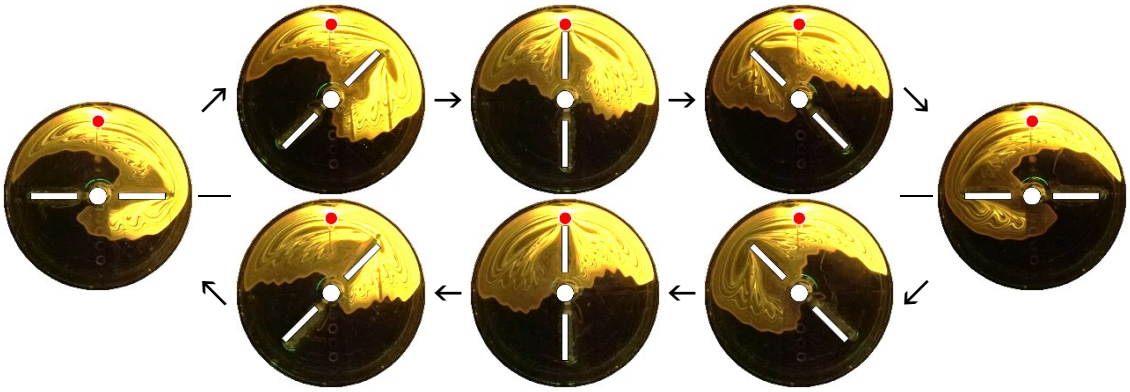

Fig. 3 Deformation of a mixing region in a single reciprocation cycle ($Re = 9.5$, 24th cycle).

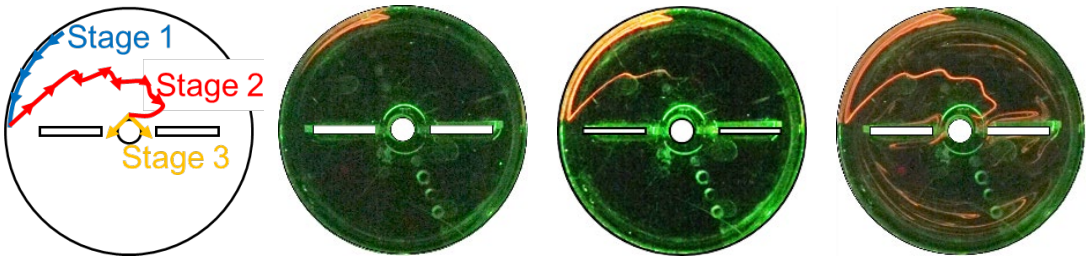

Stages 1-3 Stage 1 $(N = 8)$ Stage 2 $(N = 18)$ Stage 3 $(N = 30)$

Fig. 4 Stretching behavior of streakline; $Re = 13.8$. The stretch and contraction of the streakline are repeated along the vessel wall in Stage 1. The streakline is sucked inward from the wall, elongates on the boundary, and finally reaches the mixing shaft in Stage 2. The streakline expands in both mixing regions.

On the contrary, since the boundary seemed attached to the wall, we placed the injection point adjacent to the wall and visualized the streakline. As a result of repeated trial and error, we revealed that when the injection point is very close to the wall and slightly far from the attaching point, the tracer fluid is initially stretched along the wall, sucked inward, and finally elongated on the mixing boundary indicated by the green dashed line in Fig. 2. Fig. 4 shows the actual stretching behavior of the streakline at $Re = 13.8$ for the injection point of $r = 3.95$ cm and $\theta = 135°$. Although the shape of the boundary is dependent on Reynolds number, the stretching behavior of the streakline was similar for all the experiments ($5 < Re < 17$) and can be classified into three stages as follows. In the following section, we focus the dynamics of streakline on the boundary of mixing regions, on which tracer fluid is transported from the vessel wall to the mixing shaft without mixing with surrounding fluid in Stage 2.

3.3 Elongation of streakline along the boundary of mixing regions

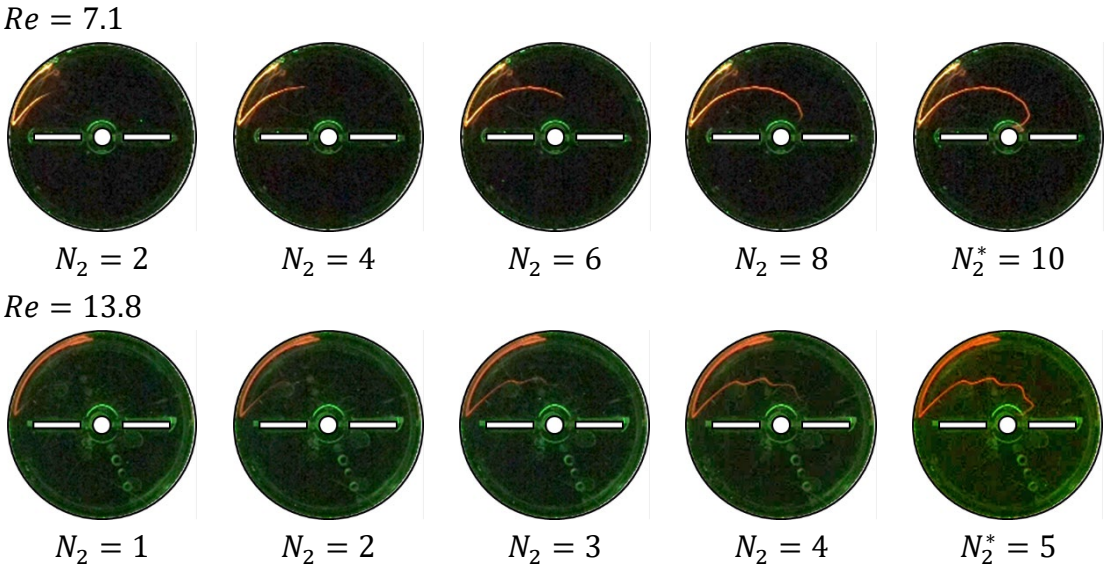

Fig. 5 Comparison of streaklines elongating on the distinct boundary.

After this, we investigated the effect of Reynold number on the elongating behavior of streakline on the boundary because the dynamics of streakline in this stage directly is related to the separation of mixing regions. Fig. 5 shows a series of images of the streakline elongating in Stage 2 at different Reynolds numbers, where N_2 is the cycle in Stage 2 and N_2^* represents the end of Stage 2. The boundary considerably deforms as the impeller plate reciprocates, but after each cycle of reciprocation, it can be seen that the streakline returns to the original shape and elongates on the boundary in a stepwise manner. Additionally, the boundary drawn by the streakline is unique and independent of the Reynolds number but becomes slightly wavy at the Reynolds number of 10 or larger. Although the shape of the boundary does not change at the Reynolds number less than 10, the elongating motion of the streakline on the boundary becomes moderate. As shown in Fig. 6, it is revealed that the number of reciprocation cycles for the streakline to elongate over the boundary in Stage 2 is inversely proportional to the Reynolds number as expressed by Eq. (3).

$$N_2^* \cdot Re = 70 \tag{3}$$

As increasing Reynolds number, the bending of the streakline becomes more noticeable and deforms vertically at a sufficiently large Reynolds number. Senda [15] reported that the hydrodynamic state becomes completely three-dimensional at the Reynolds number of 70, which corresponds to $N_2^* = 1$ in Eq. (3). The calculation suggests that at a larger Reynolds number the streakline is forced to reach the center of the vessel in less than a single reciprocation cycle, thus fluid flow turns into three-dimensional.

For the quantitative discussion on the elongating behavior, we calculate the length of the streakline at the time interval of $1/12$ s through the image analysis of pictures shown in Fig. 5. The length of streakline normalized by the vessel's inner diameter is plotted against the number of reciprocation cycles. It was found that the length of the streakline increased at a constant rate with the reciprocation cycle, and the increasing slope drastically increased at a particular cycle N_1^*, which corresponds to the

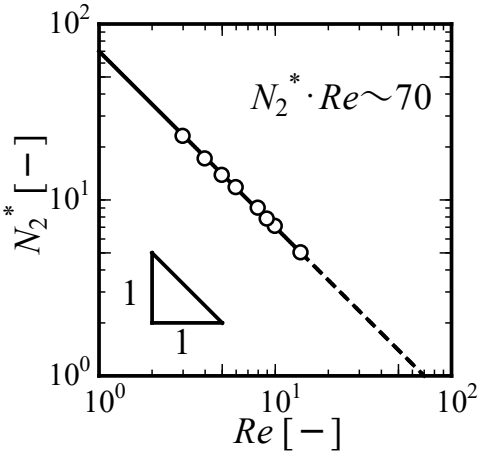

Fig. 6 Effect of Reynolds number on the cycle for stretching the streakline on the boundary from the wall to the central mixing shaft.

transition from Stage 1 to Stage 2. The increasing slope of Stage 1 was very sensitive to the injection point and not reproducible due to feeble fluid flow along the wall. In contrast, the slope in Stage 2 is large and could be measured accurately with good repeatability.

To concentrate on the elongating behavior of streakline on the boundary, we newly defined the dimensionless time in Stage 2, τ $(= t/T - N_1^*)$. Fig. 7 expresses the variations of the normalized streakline length as a function of the reciprocation cycle at

$Re = 7.1$

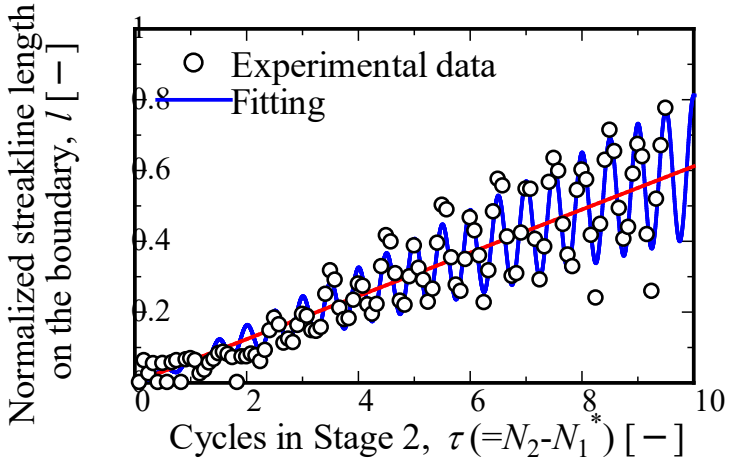

$Re = 13.8$

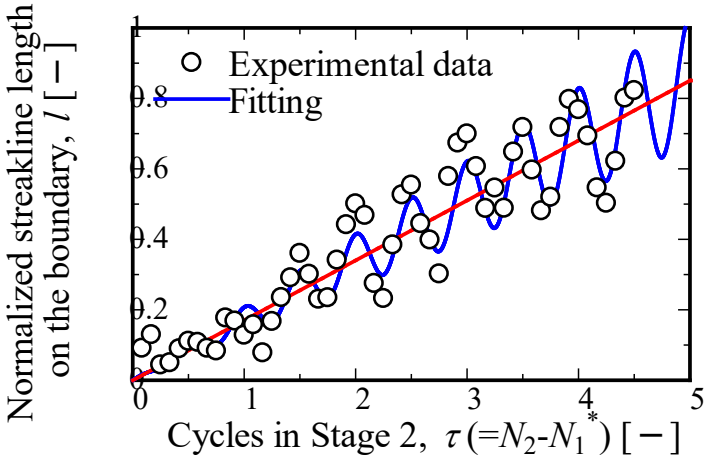

Fig. 7 Variation of streakline length on the boundary of mixing regions.

different Re. It is revealed that the streakline length increases linearly with the reciprocation cycle and additionally fluctuates at twice the frequency of the impeller reciprocation. Additionally, the fluctuating amplitude also shows a linear increase with the reciprocation cycles. Therefore, we introduced Eq. (4) to represent the variation of streakline length l, so that the streakline length was decomposed into linear and fluctuating components.

$$l = m\tau + n\ \cos(4\pi\tau) \cdot \tau \tag{4}$$

where m and n are the elongation rate of linear and fluctuating components of streakline, respectively.

Fig. 8 shows the dependence of the Reynold number on the elongation rates. The elongation rate of the fluctuating component increases linearly with the Reynolds number in the entire range investigated. The elongation rate of the linear component also has a linear relationship with the Reynolds number, but the increasing slope changes significantly at a specific Reynolds number $(Re \sim 10)$. In the previous work, we found that the power number decreased proportionally as the Reynolds number increased when

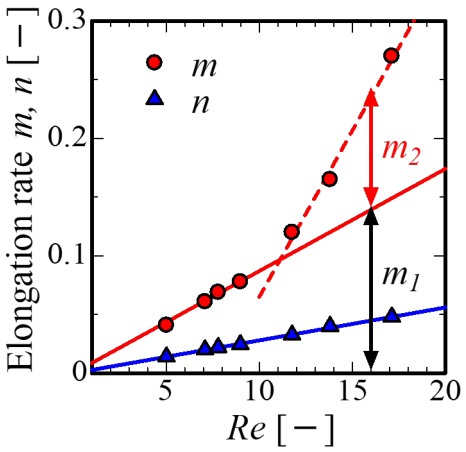

Fig. 8 Elongation rates of streakline as functions of Reynolds number.

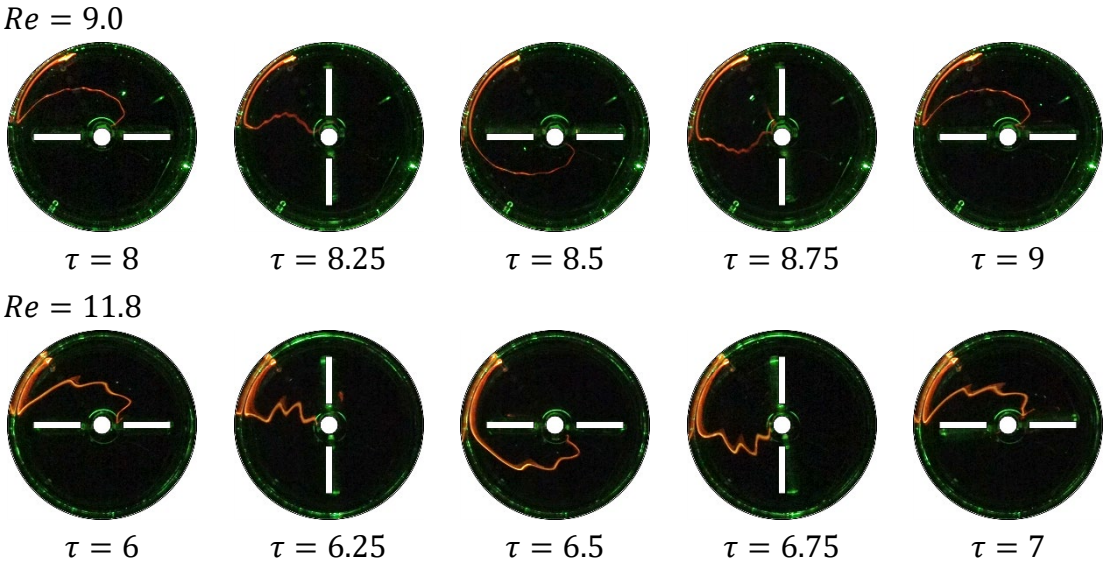

Fig. 9 Comparison of the stretching behavior streakline on the boundary around $Re = 10$.

$Re < 10$ [15]. PIV measurement of the velocity field generated by the rotationally reciprocating plate impeller shows that fluid elements will deform but essentially return to their original position at the end of each cycle since vortices formed at the impeller tips move together with the plate impeller. The mixing patterns drawn by the streakline were separated into two distinct regions, as seen in Fig. 2. Those experimental results imply that fluid flow is significantly suppressed below the critical Reynolds number ($Re \sim 10$).

To examine the transition of the elongating behavior of the streakline around $Re \sim 10$, the shape of the path of elongating streakline was observed in detail. Fig. 9 shows the comparison of the instantaneous images of the boundary visualized as the streakline in a single cycle in an early Stage 3 for $Re = 9.0$ and 11.8. In the case of $Re < 10$, the shape of the boundary was a smooth curve. In every half cycle, it seems that the boundary stretches and contracts. In other words, the relative length of the streakline to the boundary increases at a constant rate. Therefore, the streakline length at the end of the cycle increases linearly with time in Stage 2. Since the reciprocation cycle for the

streakline to reach the central region is inversely proportional to the Reynolds number in Eq. (2), the elongation rate is proportional to the Reynolds number. Additionally, assuming that the streakline is stretched and contracted uniformly over the boundary, the amplitude of fluctuation must be proportional to its length. This is the reason why the elongation rate n also has a proportional relationship with the Reynolds number.

At a larger Reynolds number, the streakline bends in every half cycle and becomes wavy. A sharp increase in m is due to the increase in the streakline length associated with the bending. However, the result cannot be explained as described in the last section. Therefore, we assumed that the linear component, m, can be divided into stretching (m_1) and bending (m_2) components, as shown in Fig. 8. At the Reynolds number below criteria, the streakline after every half cycle is elongated at a constant rate on the stable boundary. Due to the variation of the boundary length with impeller reciprocation, the streakline elongates with fluctuation. The streakline length still increases monotonously on the stable wavy boundary at the larger Reynolds number. However, the wavy boundary is repeated flattened and bent in every half cycle. This change in the boundary shape does not affect the boundary length or the elongation of the streakline. Therefore, the elongation rate m_2 reflects the effect of the shape change of the wavy boundary.

3.4 Mechanism of separation of mixing regions based on chaotic mixing theory

As described in Section 3.2, the stretching behavior of the streakline is classified into three stages. Fig. 10 illustrates the expanding behavior of the streakline in Stage 3 for $Re = 13.8$. After the streakline reaches the center, the streakline is pushed outward along both blades and enters both C-shape mixing regions. As time goes by, the shape of

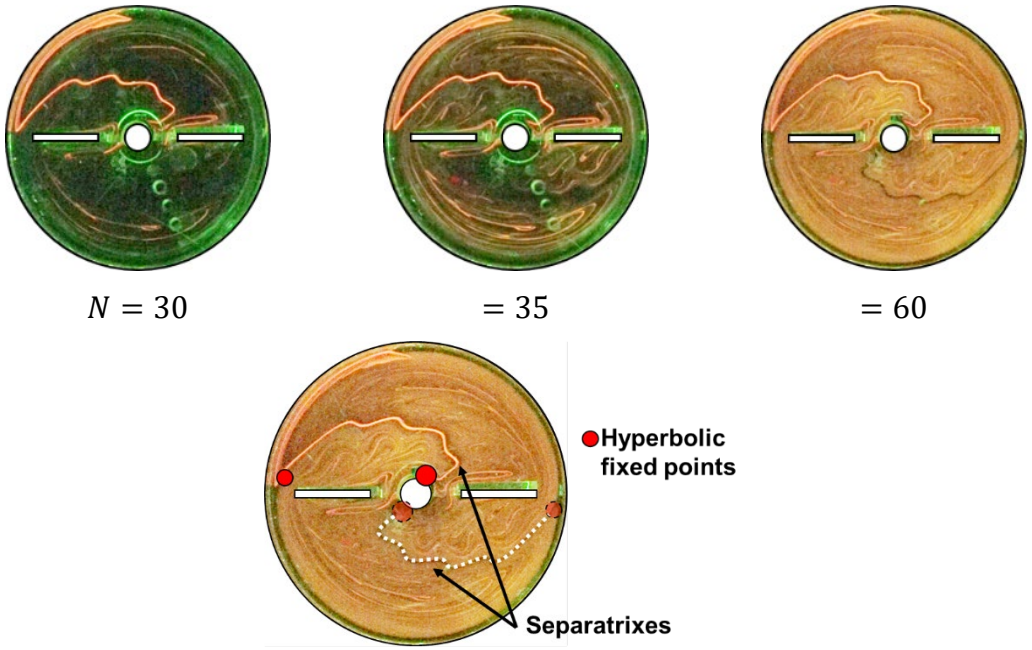

Fig. 10 Streakline patterns after Stage 3; $Re = 13.8$.

the streakline becomes indistinctive due to molecular diffusion, and both C-shape mixing regions are uniformly colored. Nevertheless, the upper-left boundary in Fig. 10 was intensely colored, while the lower-right one remains uncolored. We elucidated that tracer fluid does not mix with the fluid in both mixing regions as it is transported from the wall to the center through the boundary and that only a tiny amount of colored fluid reached the suction point of the lower-right boundary.

In specific laminar flow systems, such as Bénard cells and Moffatt eddies, fluid particles in a cell are in orbital motion, and the boundary, namely "separatrix," inhibits the exchange of fluids particles in other cells. However, when a specific perturbation is applied to the boundary condition, fluid particles in neighboring cells can cross through the hyperbolic fixed point on the perturbing separatrix [16, 17]. As shown in Fig. 9, the boundary of mixing regions attaches to the wall and the mixing shaft. The point attached to the shaft rotates back and forth with the rotation of the impeller, but from which the streakline expands into two mixing regions. Since the tracer fluid is transported from the

wall to this point along the boundary, this point can be regarded as a hyperbolic fixed point. Additionally, the other end of the boundary on the wall must be a hyperbolic fixed point because the tracer fluid is sucked in along the wall and pushed out to the central region. Therefore, it can be concluded that the path of streakline in Stage 2 is the separatrix separating the cross-section into two mixing regions.

Hence, we consider the mixing mechanism for the rotationally reciprocating anchor impeller from the analogy with that for Bénard cells with boundary perturbation. One of the two orbits in which tracer particles are transported to a hyperbolic fixed point on the wall is visualized in Stage 1. In Stage 2, tracer particles, enclosed in turnstile lobes, are conveyed to another hyperbolic point along the separatrix visualized as the boundary of mixing regions. Then, fluid particles are evenly distributed to the two mixing regions in Stage 3. For a rotationally reciprocating plate impeller, fluid motion delays in response to the impeller motion due to the separation of vortices from the impeller tip [12]. This delay can be the perturbation of separatrix since the boundary shows a wavy shape for $Re > 10$. As a result, turnstile lobes are formed by entanglement motion between stable and unstable manifolds, which was visualized in the current work as the wavy streakline on the boundary for $Re > 10$. The increase in m_2 corresponds to the increase in the area of turnstile lobes which periodically convey fluid particles to the other mixing region from the hyperbolic fixed point near the shaft. It can be concluded that the formation of a wavy boundary and the emergence of m_2 component play a crucial role in the enhancement of mixing using a reciprocating anchor impeller.

4. Conclusions

In the present work, the two-dimensional stretching process of streakline induced

by a rotationally reciprocating anchor impeller was experimentally investigated to reveal the mechanism of separation of the two mixing regions in the horizontal cross-sectional plane in the vessel.

At $Re < 17$, the cross-section of the vessel was typically separated into two distinctive mixing regions despite fluid mixing proceeded in each region, respectively. After long cycles of reciprocation, the tracer fluid injected in one of the mixing regions gradually expands into the other region, and the universal boundary was observed between the regions. This boundary was successfully visualized by injecting the tracer from a particular position, and the topology and dynamics of the streakline elongating on the boundary were discussed in detail.

The reciprocation cycles of impeller for that the streakline elongated over the boundary varies in inverse proportion to Reynolds number, which corresponds to the linear relationship between the elongation rate of streakline and Reynolds number. However, the elongation behavior of the streakline is decomposed into linear and fluctuation components. In the range of $Re < 10$, the fluctuating component is proportional to the linear one due to a smooth-shaped boundary. In contrast, the linear component at $Re > 10$ can be further divided into stretching and bending components, and the latter one is related to the wavy shape of the boundary.

Finally, the dynamics of the streakline on the boundary of mixing regions was discussed in comparison with other chaotic flows. It was concluded that the boundary is the separatrix connecting two hyperbolic fixed points near the vessel wall and the shaft, and the perturbation of the separatrix caused the wavy shape of boundary, which enhances fluid mixing by the intensive transportation of fluid particles with the help of turnstile lobes along the boundary. Since the perturbation of the separatrix increases with

increasing Reynolds number, we are convinced that the imbalance between inertial and viscous forces is a crucial factor to improve the mixing performance. It may be possible to solve this problem by modifying the shape of the impeller plate asymmetric with respect to the rotation axis, which will be investigated in the future.

References

[1] Ottino J M, Leong C W. Experiments on mixing due to chaotic advection in a cavity. J Fluid Mech 1989;209:463–499.
https://doi.org/10.1017/S0022112089003186

[2] Ottino J M. The kinematics of mixing: stretching, chaos, and transport. Cambridge: University Press; 1989.

[3] Inoue Y, Takaoka D, Okada B, Natami K, Hashimoto S, Hirata Y. Analysis of Fluid Mixing in an Agitated Vessel Based on a Streakline. Kagaku Kogaku Ronbunshu 2009;35:265–273.
https://doi.org/10.1252/kakoronbunshu.35.265

[4] Lamberto D J, Muzzio F J, Swanson P D, Tonkovich A L. Using time-dependent RPM to enhance mixing in stirred vessels. Chem Eng Sci 1996;51:733–741.
https://doi.org/10.1016/0009-2509(95)00203-0

[5] Yao W G, Sato H, Takahashi K, Koyama K. Mixing performance experiments in impeller stirred tanks subjected to unsteady rotational speeds. Chem Eng Sci 1998;57:3031–3040.
https://doi.org/10.1016/S0009-2509(98)00116-X

[6] Yek W M, Noui-Mehidi M N, Parthasarathy R, Bhattacharya S N, Wu J, Ohmura N, Nishioka N. Enhanced mixing of Newtonian fluids in a stirred vessel using impeller speed

modulation. Can J Chem Eng 2009;87:839–846.
https://doi.org/10.1002/cjce.20231
[7] Takahashi K, Kurisaka K, Sekine H. Mixing Performance Experiments in an Agitated Vessel Equipped with a Pitched Paddle Subjected to Unsteady Agitation. J Chem Eng Jpn 2011;44:852–858.
https://doi.org/10.1252/jcej.11we041
[8] Kato Y, Tada Y, Ban M, Nagatsu Y, Iwata S. Improvement of mixing Efficiencies of Conventional Impeller with Unsteady Speed in an Impeller Revolution. J Chem Eng Jpn 2005;38:688–691.
https://doi.org/10.1252/jcej.38.688
[9] Komoda Y, Inoue Y, Hirata Y. Mixing Performance by Reciprocating Disk in Cylindrical Vessel. J Chem Eng Jpn 2000;33:879–885.
https://doi.org/10.1252/jcej.33.879
[10] Hirata Y, Dote T, Komoda Y, Inoue Y. Performance of Chaotic Mixing Caused by Reciprocating a Disk in a Cylindrical Vessel. Chem Eng Res Des 2007;85:576–582.
https://doi.org/10.1205/cherd06173
[11] Komoda Y, Senda S, Takeda H, Hirata Y, Suzuki H. 2D fluid deformation induced by a rotational reciprocating plate impeller in a cylindrical vessel. Proceeding of 14th European Conference on Mixing; 2012 Sep 10–13; Warsaw, Poland.
[12] Senda S, Komoda Y, Hirata Y, Takeda H, Suzuki H, Hidema R. Characteristics of Flow Field Induced by a Rotationally Reciprocating Plate Impeller. J Chem Eng Jpn 2016;49:341–349.
https://doi.org/10.1252/jcej.15we040
[13] Senda S, Komoda Y, Hirata Y, Takeda H, S. Hiroshi, Hidema R. Fluid Deformation

Induced by a Rotationally Reciprocating Impeller. J Chem Eng Jpn 2014;47:151–158. https://doi.org/10.1252/jcej.13we081

[14] Ohmura N, Makino T, Kaise T, Kataoka K. Transition of Organized Flow Structure in a Stirred Vessel at Low Reynolds Numbers. J Chem Eng Jpn 2003;36:1458–1463. https://doi.org/10.1252/jcej.36.1458

[15] Senda S. Fluid Mixing induced by a Rotationally Reciprocating Impeller (in Japanese) [PhD Dissertation]. Kobe: Kobe University; 2015.

[16] Camassa R, Wiggins S. Chaotic advection in a Rayleigh-Bénard flow. Phys Rev A 1991;43:774–797. https://link.aps.org/doi/10.1103/PhysRevA.43.774

[17] Ryrie S. Mixing by chaotic advection in a class of spatially periodic flows. J Fluid Mech 1992;236:1–26. https://doi.org/10.1017/S0022112092001319